universe

MDPI

Article

Scaling Invariance of Perturbations in *k*-Inflation Models

Neven Bilić [1,*], Dragoljub D. Dimitrijević [2], Goran S. Djordjević [2], Milan Milošević [2] and Marko Stojanović [3]

[1] Division of Theoretical Physics, Rudjer Bošković Institute, 10000 Zagreb, Croatia
[2] Department of Physics, University of Niš, 18000 Niš, Serbia; ddrag@pmf.ni.ac.rs (D.D.D.); gorandj@junis.ni.ac.rs (G.S.D.); milan.milosevic@pmf.edu.rs (M.M.)
[3] Faculty of Medicine, University of Niš, 18000 Niš, Serbia; marko.stojanovic@pmf.edu.rs
* Correspondence: bilic@irb.hr

Abstract: We study the background and perturbations in *k*-essence inflation models and show that a general *k*-essence exhibits a simple scaling property. In particular, we study two classes of *k*-inflation models with the potential characterized by an inflection point. We demonstrate that these models enjoy scaling properties that could be used to redefine input parameters so that the perturbations spectra satisfy the correct normalization at the CMB pivot scale. The background and perturbation equations are integrated numerically for two specific models.

Keywords: *k*-essence; inflation; cosmological perturbations

Academic Editor: Kazuharu Bamba

Received: 13 February 2025
Revised: 1 April 2025
Accepted: 6 April 2025
Published: 9 April 2025

Citation: Bilić, N.; Dimitrijević, D.D.; Djordjević, G.S.; Milošević, M.; Stojanović, M. Scaling Invariance of Perturbations in *k*-Inflation Models. *Universe* **2025**, *11*, 128. https://doi.org/10.3390/universe11040128

1. Introduction

The origin of the field driving inflation is still unknown and subject to speculation. The models in which the kinetic term has a noncanonical form are usually referred to as *k*-essence [1] or, in the context of inflation, *k*-inflation models [2]. As argued by Armendáriz-Picón, Damour, and Mukhanov [2], a field theory with noncanonical kinetic terms can be motivated by a low-energy realization of string theory. Suppose we only have gravity and some moduli field φ (e.g., the dilaton) in string theory. Then, α' corrections (due to the massive modes of the string) generate a series of higher-derivative terms in the low-energy effective action, while string-loop corrections generate the non-trivial moduli dependence of the coefficients of the various kinetic terms. Passing from the string to the Einstein frame, one obtains the effective Lagrangian of the form $\mathcal{L} = K(\varphi)X + L(\varphi)X^2 + \cdots$, where $X = g^{\mu\nu}\varphi_{,\mu}\varphi_{,\nu}$. More details can be found in Ref. [2].

A distinguished feature of *k*-essence models is that even without any potential energy term, a general class of non-standard kinetic-energy terms can drive an inflationary evolution of the same type as the usually considered potential-driven inflation. For example, a simple *k*-essence model with Lagrangian $\mathcal{L} = -A\sqrt{1-X}$ in the slow-roll regime produces an accelerated expansion, i.e., a quasi-de Sitter evolution. In the cosmological context, this model is equivalent to the so-called Chaplygin gas [3] and serves as a prototype model for dark matter/dark energy unification [4]. Promoting the constant A to a field-dependent potential, this model becomes the Tachyon model—a particularly important *k*-essence model extensively studied in the literature [5–16].

In this work, we study the *k*-essence using the Hamiltonian formalism for background field equations. We show that a general *k*-essence exhibits a simple scaling property under the condition that the Lagrangian admits a multiplication by a constant. We then focus our studies to two broad classes of *k*-essence.

In class A, the Lagrangian is of the form $(X/2)^\alpha - U(\varphi)$, where $\alpha \geq 1$ is a constant, $X = g^{\mu\nu}\varphi_{,\mu}\varphi_{,\nu}$, and U is a smooth function of the field φ. A typical representative of this

class is the model proposed by Papanikolaou, Lymperis, Lola, and Saridakis [17], which we will refer to as the PLLS model. Their potential is a function of the field with an inflection point. The potentials with inflection or near the inflection point always lead to a peak in the power spectrum of curvature perturbations on scales below the CMB pivot scale. Enhanced cosmological perturbations could collapse into primordial black holes (BHs) [18–20].

Class B is represented by the Lagrangian of the form $-U(\varphi)F(X)$, where F is a smooth function of X. A typical representative of this class is the Tachyon model with a Lagrangian of the Dirac-Born-Infeld (DBI) form

$$\mathcal{L}_{\rm DBI} = -U(\varphi)\sqrt{1-X}. \tag{1}$$

Our interest in the Tachyon model is mostly motivated by low-energy string theory. The existence of tachyons in the perturbative spectrum of string theory shows that the perturbative vacuum is unstable. This instability implies that there is a real vacuum to which a tachyon field φ tends [21]. The foundations of this process are given by a model of effective field theory [22,23] with the Lagrangian of the DBI form. A similar Lagrangian appears in the so-called brane inflation models [24]. In these models, inflation is driven by the motion of a D3-brane in a warped throat region of a compact space, and the DBI field corresponds to the position of the D3-brane. To see how the tachyon Lagrangian appears through the dynamics of a 3-brane (see Ref. [25] for details), consider a 3-brane moving in the 4+1-dimensional bulk spacetime with coordinates X^a, $a = 0, 1, 2, 3, 4$ and line element

$$ds^2_{(5)} = G_{ab}dX^a dX^b = \chi(z)^2(g_{\mu\nu}dx^\mu dx^\nu - dz^2). \tag{2}$$

The points on the brane are parameterized by $X^a(x^\mu)$, $\mu = 0, 1, 2, 3$, where x^μ represents the coordinates on the brane. The brane action is given by

$$S_{\rm br} = -\sigma \int d^4x \sqrt{-\det(G_{ab}X^a_{,\mu}X^b_{,\nu})}\,, \tag{3}$$

where σ is the brane tension. Taking the Gaussian normal parameterization $X^a(x^\mu) = (x^\mu, z(x^\mu))$, a straightforward calculation of the determinant yields the brane action Lagrangian in the form (1), in which the role of the field is played by the extra coordinate z with $X = g^{\mu\nu}z_{,\mu}z_{,\nu}$ and $U(z) = \sigma\chi(z)^4$.

We will demonstrate that both A and B models enjoy scaling properties that one can use to tune the model parameters and initial values without affecting the shape of the curvature perturbation spectrum. The tuning of the input parameters is often necessary to achieve the desired properties of the perturbation spectrum, but this inevitably changes the normalization of the spectrum if one adheres to the Bunch–Davies asymptotic condition. However, owing to the scaling properties, one can redefine the input parameters so that the spectrum keeps its shape and satisfies the correct normalization at the CMB pivot scale.

The remainder of the paper is organized as follows. In Section 2, we give an overview of the covariant Hamilton formalism. In Section 3, we consider two classes of k-essence and present the formalism that describes the background evolution. In Section 4, we investigate the spectra of curvature perturbations for these two classes of models. In the last section, Section 5, we summarize our main results and lay out our conclusions.

Notation

We use the metric signature $(+,-,-,-)$. For convenience, we introduce a length scale ℓ so that $\ell \gg 1/M_{\rm Pl}$, where $M_{\rm Pl} = \sqrt{1/(8\pi G)}$ is the reduced Planck mass. By $\mathcal{L}$ and $\mathcal{H}$, we denote the Lagrangian and Hamiltonian, multiplied by ℓ^4, so that our Lagrangian and Hamiltonian are dimensionless. By φ and ϕ, we denote the scalar fields connected by $\varphi = \ell^2\phi$ and have the dimension of length and mass, respectively.

2. Hamilton Formalism

For a general (dimensionless) scalar field Lagrangian $\mathcal{L}(\varphi_{,\mu}, \varphi)$, the (dimensionless) covariant Hamiltonian $\mathcal{H}(\eta^\mu, \varphi)$ is related to $\mathcal{L}$ through the Legendre transformation

$$\mathcal{H}(\eta^\mu, \varphi) = \eta^\mu \varphi_{,\mu} - \mathcal{L}(\varphi_{,\mu}, \varphi), \tag{4}$$

with conjugate variables satisfying the conditions

$$\varphi_{,\mu} = \frac{\partial \mathcal{H}}{\partial \eta^\mu}, \tag{5}$$

$$\eta^\mu = \frac{\partial \mathcal{L}}{\partial \varphi_{,\mu}}. \tag{6}$$

From (4), we have

$$\frac{\partial \mathcal{H}}{\partial \varphi} = -\frac{\partial \mathcal{L}}{\partial \varphi}. \tag{7}$$

By making use of Equations (6), (7), and the Euler–Lagrange equation

$$\left(\frac{\partial \mathcal{L}}{\partial \varphi_{,\mu}}\right)_{;\mu} = \frac{\partial \mathcal{L}}{\partial \varphi}, \tag{8}$$

we find

$$\eta^\mu{}_{;\mu} = -\frac{\partial \mathcal{H}}{\partial \varphi}. \tag{9}$$

Equations (5) and (9) are the covariant Hamilton equations.

The most general scalar field Lagrangian is a function of the form $\mathcal{L} = \mathcal{L}(X, \varphi)$, where

$$X = g^{\mu\nu}\varphi_{,\mu}\varphi_{,\nu}. \tag{10}$$

This type of Lagrangian represents the so-called *k*-essence theory. In cosmological applications, the kinetic term X is assumed positive. From (6), it follows that the quantity

$$\eta^2 = g_{\mu\nu}\eta^\mu\eta^\nu = 4X(\mathcal{L}_X)^2 \tag{11}$$

is also positive. Here, the subscript $_X$ denotes a derivative with respect to X. Then, one can introduce the four-velocity

$$u_\mu = \frac{g_{\mu\nu}\eta^\nu}{\eta} = \epsilon\frac{\varphi_{,\mu}}{\sqrt{X}}, \tag{12}$$

where ϵ is $+1$ or -1, according to whether $\varphi_{,0}$ is, respectively, positive or negative. This choice of ϵ guaranties that u_0 is always positive. The requirement of positivity of u_0 is natural in the context of FRW cosmology, where we require that the expansion rate

$$H \equiv \frac{1}{3}u^\mu{}_{;\mu} \tag{13}$$

equals $\dot{a}/a$ in a comoving frame. The quantity η in (12) is a square root of (11). The sign of the root is fixed by

$$\eta \equiv 2\epsilon\sqrt{X}\mathcal{L}_X = \epsilon\frac{\partial \mathcal{L}}{\partial \sqrt{X}}, \tag{14}$$

which follows from (11) and (12). Here, and throughout the paper, we assume $\sqrt{X} \geq 0$. Hence, η can be positive or negative depending on the signs of ϵ and $\mathcal{L}_X$.

In a k-essence type of theory, the Hamiltonian is a function of $\eta^2 = g_{\mu\nu}\eta^\mu\eta^\nu$ and φ. One can see this as follows. First, using (4) and (6), one can express $\mathcal{H}$ as a function of X and φ,

$$\mathcal{H} = 2X\mathcal{L}_X - \mathcal{L}. \tag{15}$$

Then, from (14), it follows that X is an implicit function of η^2 and φ, which we can (in principle) solve for X to obtain $X = X(\eta^2, \varphi)$. Then, we can plug in this solution into the right-hand side of (15) to obtain $\mathcal{H} = \mathcal{H}(\eta^2, \varphi)$. Besides, one can show that the Lagrangian can be expressed as a function of η^2 and φ

$$\mathcal{L} = \eta\frac{\partial\mathcal{H}}{\partial\eta} - \mathcal{H}, \tag{16}$$

which follows from (4), (5), and the definition $\eta^2 = g_{\mu\nu}\eta^\mu\eta^\nu$.

Using (5)–(8) and (10)–(12), we can write the Hamilton equations in the standard form

$$\dot{\varphi} = \frac{\partial\mathcal{H}}{\partial\eta}, \tag{17}$$

$$\dot{\eta} + 3H\eta = -\frac{\partial\mathcal{H}}{\partial\varphi}, \tag{18}$$

where we have used the usual notation $\dot{f} \equiv u^\mu f_{,\mu}$ and the definition of the expansion rate. As usual, we identify the Lagrangian and Hamiltonian with the pressure p and energy density ρ, respectively. Then, in a cosmological context, the Hubble expansion rate and its time derivative can be related to the Hamiltonian and Lagrangian. Using the Friedmann equations, we find

$$H^2 = \frac{\mathcal{H}}{3\ell^4 M_{\rm Pl}^2}, \tag{19}$$

$$\dot{H} = -\frac{\mathcal{L} + \mathcal{H}}{2\ell^4 M_{\rm Pl}^2} = -\frac{\eta\mathcal{H}_{,\eta}}{2\ell^4 M_{\rm Pl}^2}. \tag{20}$$

It is sometimes convenient to express Equations (17) and (18) in terms of the Lagrangian. With the help of (7), (11), and (15), we find

$$\dot{\varphi} = \frac{\eta}{2\mathcal{L}_X}, \tag{21}$$

$$\dot{\eta} + 3H\eta = \frac{\partial\mathcal{L}}{\partial\varphi}. \tag{22}$$

It is worth noting that Equation (4) can be written as a Legendre transformation

$$\mathcal{H}(\eta, \varphi) = \eta\varphi_{,0} - \mathcal{L}(\varphi_{,0}, \varphi), \tag{23}$$

with two conjugate variables $\varphi_{,0} \equiv \epsilon\sqrt{X}$ and η satisfying

$$\varphi_{,0} = \frac{\partial\mathcal{H}}{\partial\eta}, \tag{24}$$

$$\eta = \frac{\partial\mathcal{L}}{\partial\varphi_{,0}}. \tag{25}$$

Equation (24) is the first Hamilton equation equivalent to (17). The second Hamilton equation equivalent to (18) can be obtained from the Euler–Lagrange equation

$$\frac{1}{\sqrt{-g}}\left(\sqrt{-g}\frac{\partial\mathcal{L}}{\partial\varphi_{,0}}\right)_{,0}=\frac{\partial\mathcal{L}}{\partial\varphi}, \tag{26}$$

with (25) and (7). Note also that Equation (16) follows directly from (23) and (24).

A Few Useful Relations

The speed of sound squared can be expressed either as a function of X and φ,

$$c_s^2\equiv\left.\frac{\partial p}{\partial\rho}\right|_{\varphi}=\frac{\mathcal{L}_X}{\mathcal{H}_X}=\frac{\mathcal{L}_X}{\mathcal{L}_X+2X\mathcal{L}_{XX}}, \tag{27}$$

or as a function of η and φ,

$$c_s^2=\frac{\mathcal{L}_{,\eta}}{\mathcal{H}_{,\eta}}=\frac{\eta\mathcal{H}_{,\eta\eta}}{\mathcal{H}_{,\eta}}. \tag{28}$$

Here, the subscripts $,\eta$ and $,\eta\eta$ denote, respectively, the first- and second-order partial derivatives with respect to η.

The first slow-roll parameter ε_1 can be expressed in terms of η and φ, using the second Friedmann Equation (20), yielding

$$\varepsilon_1\equiv-\frac{\dot{H}}{H^2}=\frac{3}{2}\frac{\eta\mathcal{H}_{,\eta}}{\mathcal{H}}. \tag{29}$$

3. k-Essence Inflation Models

Inflation models based on a scalar field theory with noncanonical kinetic terms are usually referred to as k-essence [1]. For a general k-essence of the form $\mathcal{L}=\mathcal{L}(X,\lambda\varphi)$, where λ is a parameter of the dimension of the mass, one can demonstrate simple scaling properties which can be useful for tuning the model parameters and initial values. First, we introduce the e-fold number

$$N=\int dtH, \tag{30}$$

and rewrite the Hamilton Equations (17) and (18) as differential equations with respect to N

$$\frac{d\varphi}{dN}=\frac{1}{H}\frac{\partial\mathcal{H}}{\partial\eta}, \tag{31}$$

$$\frac{d\eta}{dN}+3\eta=-\frac{1}{H}\frac{\partial\mathcal{H}}{\partial\varphi}, \tag{32}$$

It may easily be shown that Equations (31) and (32) are invariant under the following simultaneous rescaling

$$\begin{aligned}&\mathcal{L}\to c_0^{-1}\mathcal{L},\quad\lambda\to c_0^{-1/2}\lambda,\\&\varphi\to c_0^{1/2}\varphi,\quad\eta\to c_0^{-1}\eta,\end{aligned} \tag{33}$$

where c_0 is an arbitrary positive constant.

Next, we consider two popular classes of k-essence, described as follows.

3.1. Model A

This class of models is defined by the Lagrangian

$$\mathcal{L}=\left(\frac{X}{2}\right)^{\alpha}-U(\lambda\varphi), \tag{34}$$

where $\alpha > 1$ is a dimensionless constant, $\lambda > 0$ is a constant of dimension of mass, and φ is the field of dimension of length. The physical field ϕ, related to φ via

$$\varphi = \ell^2 \phi, \tag{35}$$

has the usual dimension of mass. We assume that the kinetic term $X \equiv g^{\mu\nu}\varphi_{,\mu}\varphi_{,\nu}$ is positive and that U is a smooth dimensionless function of its argument. As described in Section 2, the corresponding Hamiltonian is obtained by the Legendre transformation (15) yielding

$$\mathcal{H} = (2\alpha - 1)\left(\frac{X}{2}\right)^{\alpha} + U(\lambda\varphi). \tag{36}$$

Then, the Hubble expansion rate H is given by (19) and the speed of sound by

$$c_s^2 \equiv \frac{\mathcal{L}_X}{\mathcal{H}_X} = \frac{1}{2\alpha - 1}. \tag{37}$$

Now, we introduce the conjugate momentum and its magnitude η as described in Section 2. In this model, X can be expressed as an explicit function of η. By making use of (34) and (14), we find

$$\frac{X}{2} = \left(\frac{\eta^2}{2\alpha^2}\right)^{1/(2\alpha-1)}. \tag{38}$$

Then, we obtain the Hamiltonian expressed in terms of φ and η as

$$\mathcal{H} = (2\alpha - 1)\left(\frac{\eta^2}{2\alpha^2}\right)^{\alpha/(2\alpha-1)} + U(\lambda\varphi). \tag{39}$$

The first slow-roll parameter is given by

$$\varepsilon_1 = \frac{\mathcal{L} + \mathcal{H}}{2\ell^4 M_{\rm Pl}^2 H^2} = \frac{3\alpha\left[\eta^2/(2\alpha^2)\right]^{\alpha/(2\alpha-1)}}{(2\alpha - 1)\left[\eta^2/(2\alpha^2)\right]^{\alpha/(2\alpha-1)} + U(\lambda\varphi)}. \tag{40}$$

The end of inflation is determined by the condition $1 - \varepsilon_1 \simeq 0$.

The dynamics are governed by the Hamilton Equations (31) and (32), defined for a general k-essence. In this model, we find

$$\frac{d\varphi}{dN} = \frac{\eta}{\alpha H}\left(\frac{\eta^2}{2\alpha^2}\right)^{(1-\alpha)/(2\alpha-1)}, \tag{41}$$

$$\frac{d\eta}{dN} = -3\eta - \frac{1}{H}\frac{\partial U}{\partial \varphi}, \tag{42}$$

where H is the Hubble rate

$$H = \frac{1}{\sqrt{3}\,\ell^2 M_{\rm Pl}}\left[(2\alpha - 1)\left(\frac{\eta^2}{2\alpha^2}\right)^{\alpha/(2\alpha-1)} + U(\lambda\varphi)\right]^{1/2}. \tag{43}$$

The scaling property of the general k-essence described by (33) does not apply to this model, since we do not have the freedom to rescale the kinetic part. Nevertheless, it may be shown that the above Hamilton equations are invariant under the following simultaneous rescaling of the potential parameters and fields

$$U \to c_0^{-1} U, \quad \lambda \to c_0^{(1-\alpha)/(2\alpha)}\lambda,$$

$$\varphi \to c_0^{(\alpha-1)/(2\alpha)}\varphi, \quad \eta \to c_0^{(1-2\alpha)/(2\alpha)}\eta. \tag{44}$$

The Hubble rate scales according to $H \to c_0^{-1/2}H$, and the rescaled Hamilton equations retain the form (41) and (42).

Note that any canonical single-field inflation model enjoys the above scaling property. On the other hand, in multifield inflation models, this type of scaling is not a general property. However, it is not excluded that some canonical multifield inflation models obey a similar scaling property, depending on the particulars of the potential.

The Klein-Gordon Equation

Instead of Hamilton's equations, one can use the second-order Klein-Gordon (KG) equation, i.e., the field equation of motion. This equation can be obtained directly from the Lagrangian or by combining Equations (41) and (42). Either way, one finds

$$\varphi'' + \left(\frac{3}{2\alpha-1} - \varepsilon_1\right)\varphi' + \frac{1}{U}\frac{dU}{d\varphi}\frac{3\alpha-(2\alpha-1)\varepsilon_1}{2\alpha(2\alpha-1)\varepsilon_1}\varphi'^2 = 0, \tag{45}$$

where

$$\varepsilon_1 = \frac{\alpha}{\ell^2 H^2}\left(\frac{H^2\varphi'^2}{2}\right)^{\alpha}, \tag{46}$$

and H is a solution to

$$\ell^2 H^2 = \frac{1}{3}\left[(2\alpha-1)\left(\frac{H^2\varphi'^2}{2}\right)^{\alpha} + U(\lambda\varphi)\right]. \tag{47}$$

Here, and from here on, the prime $'$ denotes a derivative with respect to N.

The expression (47) is an algebraic equation for the unknown H^2 and is generally not solvable unless α is an integer < 5. For a fractional α, e.g., $\alpha = 1.5$ and 1.3 used in [17], the KG equation involves an implicit function of $H(\varphi, \varphi')$, which requires a cumbersome numerical procedure. However, one can simplify the numerical procedure by calculating H via the 2nd Friedmann equation. Then, we need to solve the differential equation

$$H' = -\frac{\alpha}{\ell^2 H}\left(\frac{H^2\varphi'^2}{2}\right)^{\alpha}, \tag{48}$$

in addition to (45). As a part of this procedure, one needs to solve the algebraic Equation (47) only at the initial point $N_{\rm in}$ to find the initial value $H_{\rm in}$ as a function of initial $\varphi_{\rm in}$ and $\varphi'_{\rm in}$. In any case, we see that the Hamiltonian approach has a certain advantage, although the pair of Hamilton Equations (41) and (42) are equivalent to Equation (45).

3.2. Model B

The Lagrangian in this class of models is of the form

$$\mathcal{L} = -U(\lambda\varphi)F(X). \tag{49}$$

As in Model A, λ is a positive constant of the dimension of mass and φ is the field of the dimension of length. We assume that F is a smooth functions of $X \equiv g^{\mu\nu}\varphi_{,\mu}\varphi_{,\nu} > 0$, and U is an arbitrary smooth dimensionless functions of its argument. The corresponding Hamiltonian is given by

$$\mathcal{H} = U(\lambda\varphi)(F(X) - 2XF_X(X)). \tag{50}$$

As in Model A, we identify the Lagrangian and Hamiltonian with the pressure p and energy density ρ, respectively. Then, the Hubble rate is defined by (19), the speed of sound by

$$c_s^2 \equiv \frac{\mathcal{L}_X}{\mathcal{H}_X} = \frac{F_X}{F_X + 2XF_{XX}}, \tag{51}$$

and the first slow-roll parameter by

$$\varepsilon_1 \equiv -\frac{\dot{H}}{H^2} = \frac{\mathcal{L} + \mathcal{H}}{2\ell^4 M_{\rm Pl}^2 H^2} = \frac{3XF_X}{2XF_X - F}. \tag{52}$$

As before, we introduce the conjugate momentum and its magnitude η. According to Equation (11), X is an implicit function of the field φ and the conjugate field η

$$4X(F_X)^2 = \frac{\eta^2}{U(\lambda\varphi)^2}. \tag{53}$$

Then, the Hamilton Equations (17) and (18), expressed as differential equations with respect to N in this model, are

$$\frac{d\varphi}{dN} = -\frac{1}{H}\frac{\eta}{2UF_X}, \tag{54}$$

$$\frac{d\eta}{dN} = -3\eta - \frac{F}{H}\frac{\partial U}{\partial \varphi}. \tag{55}$$

It is understood that the variable X in Equations (54) and (55) is an implicit function of η^2 and φ via Equation (53). In principle, X may be expressed as an explicit function of η^2 and φ by solving (53) for X.

The scaling property of the general k-essence described by (33) applies directly to this model, since we have the freedom to rescale the potential, and rescaling the potential implies identical rescaling of the Lagrangian. Hence, Model B exhibits the invariance of its Hamilton equations under

$$\begin{aligned} U \to c_0^{-1}U, \quad \lambda \to c_0^{-1/2}\lambda, \\ \varphi \to c_0^{1/2}\varphi, \quad \eta \to c_0^{-1}\eta. \end{aligned} \tag{56}$$

Clearly, Equation (53) renders X, F, and F_X invariant under this rescaling, whereas the Hubble rate scales according to $H \to c_0^{-1/2}H$. Then, the rescaled Hamilton equations retain the form (54) and (55) with no dependence on c_0.

The Tachyon Model

The most popular model that belongs to class B is the Tachyon model with $F(X) = \sqrt{1-X}$ in Equation (49) and the Lagrangian

$$\mathcal{L} = -U(\lambda\varphi)\sqrt{1-X}. \tag{57}$$

Using this and (53), we obtain X as an explicit function of the fields φ and η

$$X = \frac{\eta^2}{U^2 + \eta^2}. \tag{58}$$

The Hamiltonian can be expressed as a function of either X or η^2,

$$\mathcal{H} = \frac{U}{\sqrt{1-X}} = \sqrt{U^2 + \eta^2}, \tag{59}$$

and the Hamilton equations become

$$\frac{d\varphi}{dN} = \frac{\eta}{H\sqrt{U^2+\eta^2}}, \tag{60}$$

$$\frac{d\eta}{dN} = -3\eta - \frac{U}{H\sqrt{U^2+\eta^2}}\frac{\partial U}{\partial \varphi}, \tag{61}$$

where the Hubble rate is given by

$$H^2 = \frac{\sqrt{U^2+\eta^2}}{3\ell^4 M_{\rm Pl}^2}. \tag{62}$$

The slow-roll parameter and the sound speed squared can be expressed as

$$\varepsilon_1 = \frac{3}{2}X = \frac{3}{2}\frac{\eta^2}{U^2+\eta^2}, \tag{63}$$

$$c_{\rm s}^2 = 1 - X = \frac{U^2}{U^2+\eta^2} = 1 - \frac{2}{3}\varepsilon_1. \tag{64}$$

4. Curvature Perturbations

We start from the first-order differential equations of Garriga and Mukhanov [26], expressed in the form [16,27]

$$a\dot{\xi}_q = z^2 c_{\rm s}^2 \zeta_q, \tag{65}$$

$$a\dot{\zeta}_q = -z^{-2} q^2 \xi_q, \tag{66}$$

where q is the comoving wavenumber. The quantity z can be expressed in different ways, as follows:

$$z^2 = \frac{a^2(p+\rho)}{H^2 c_{\rm s}^2} = \frac{2M_{\rm Pl}^2 a^2 \varepsilon_1}{c_{\rm s}^2} = \frac{a^2 \eta \mathcal{H}_{,\eta}}{\ell^4 H^2 c_{\rm s}^2} = \frac{a^2 \mathcal{H}_{,\eta}^2}{\ell^4 H^2 \mathcal{H}_{,\eta\eta}}. \tag{67}$$

Here, the subscripts $,\eta$ and $,\eta\eta$ denote, respectively, the first and second-order partial derivatives with respect to η.

4.1. Mukhanov–Sasaki Equation

It is convenient to substitute the e-fold number N for t using $dt = dN/H$ and express Equations (65)–(66) as differential equations with respect to N. Then, combining the obtained equations, one can derive the Mukhanov–Sasaki second-order differential equation

$$\frac{d^2\zeta_q}{dN^2} + \left(3 + \varepsilon_2 - \varepsilon_1 - 2\frac{c_{\rm s}'}{c_{\rm s}}\right)\frac{d\zeta_q}{dN} + \frac{c_{\rm s}^2 q^2}{a^2 H^2}\zeta_q = 0, \tag{68}$$

which is equivalent to the set (65)–(66) with (67). Here, the second slow-roll parameters are defined as $\varepsilon_2 = \dot{\varepsilon}_1/(H\varepsilon_1)$.

The perturbations travel at the speed of sound, and their horizon is the acoustic horizon with radius $c_{\rm s}/H$. At the acoustic horizon, the perturbations with the comoving wavenumber q satisfy the horizon crossing relation

$$a(N)H(N) = c_{\rm s}(N)q. \tag{69}$$

In the slow-roll regime, the perturbations are conserved once they cross the horizon from the subhorizon to the superhorizon region. This can be seen as follows. In the superhorizon

region, i.e., when the physical wavelength of the perturbation a/q is much bigger than the sound horizon c_s/H, the last term on the left-hand side of Equation (68) can be neglected. Then, in the slow-roll approximation, the contribution of the terms proportional to ε_1, ε_2, and $\dot{c}_s$ can also be neglected, and the equation takes the form $\zeta_q'' + 3\zeta_q' = 0$ with solution $\zeta_q = C_1 + C_2 \exp(-3N)$, where C_1 and C_2 are constants. As we shall shortly see, the horizon crossing happens at a relatively large q-dependent N of the order $N_q \sim 7 + \ln q/q_{\rm CMB}$, where $q_{\rm CMB}$ is the CMB pivot scale. Hence, the curvature perturbations ζ_q are approximately constant at a large N, once they cross the horizon and enter the superhorizon region where $a(N)H(N) > c_s(N)q$, $N > N_q$.

The power spectrum of the curvature perturbations is given by

$$\mathcal{P}_S(q) = \frac{q^3}{2\pi^2}|\zeta_q(N_q)|^2, \tag{70}$$

where $\zeta_q(N_q)$ is the solution to Equation (68) taken at the point N_q, which for a given q satisfy (69). The curvature perturbation spectrum needs to satisfy the Harrison–Zeldovich spectrum near $q = q_{\rm CMB} = 0.05\ {\rm Mpc}^{-1}$

$$\mathcal{P}_S(q) = A_s\left(\frac{q}{q_{\rm CMB}}\right)^{n_s-1}, \tag{71}$$

where $A_s = (2.10 \pm 0.03) \times 10^{-9}$. Since the Mukhanov–Sasaki Equation (68) is linear, the normalization of ζ_q can be fixed by the requirement

$$\mathcal{P}_S(q_{\rm CMB}) = \frac{q_{\rm CMB}^3}{2\pi^2}|\zeta_{q_{\rm CMB}}(N_{q_{\rm CMB}})|^2 = A_s = 2.1 \cdot 10^{-9}. \tag{72}$$

We need to integrate Equation (68) in conjunction with the Hamilton equations in the subhorizon region up to N_q, where N_q satisfies the horizon crossing relation $aH = c_s q$. The appropriate q-dependent initial point is set in the deep subhorizon region where $a_{\rm in}H_{\rm in} << c_s q$. Hence, for each wavenumber q, we start at a q-dependent $N_{{\rm in},q}$ such that

$$a_{{\rm in},q}H_{{\rm in},q} = \beta c_{s,q} q, \tag{73}$$

where β is a small parameter, e.g., $\beta = 0.01$ as proposed in Ref. [28]. Here, $H_{{\rm in},q} = H(N_{{\rm in},q})$, $c_{s,q} = c_s(N_{{\rm in},q})$, and

$$a_{{\rm in},q} = a_0 e^{N_{{\rm in},q} - N_0}, \tag{74}$$

where a_0 is the cosmological scale factor at $N = N_0$. In particular, for $q = q_{\rm CMB}$,

$$a_0 e^{N_{{\rm in},q_{\rm CMB}} - N_0} H_{{\rm in},q_{\rm CMB}} = \beta c_{s,q_{\rm CMB}} q_{\rm CMB}. \tag{75}$$

Owing to the N-translation invariance of the background equations, we could choose the origin of inflation at an arbitrary N_0 such that the corresponding $q_0 < q_{\rm CMB}$, i.e., we set

$$a_0 H_0 = \beta c_{s0} q_0 = \epsilon c_{s0} q_{\rm CMB}, \tag{76}$$

where $H_0 = H(N_0)$, $c_{s0} = c_s(N_0)$, and the quantity ϵ is a small parameter, $\epsilon < \beta$, e.g., $\epsilon = 0.001$. Equation (76) means that the perturbation with $q = q_{\rm CMB}$ will cross the horizon at $N = N_{q_{\rm CMB}}$, which satisfies the condition

$$\epsilon e^{-N_0} \frac{e^{N_{q_{\rm CMB}}} H(N_{q_{\rm CMB}})}{H_0} \frac{c_{s0}}{c_s(N_{q_{\rm CMB}})} = 1. \tag{77}$$

For an arbitrary q, the horizon crossing relation

$$a_0 e^{N-N_0} H(N) = c_s(N) q, \tag{78}$$

combined with (76), may be written as

$$\frac{q}{q_{\rm CMB}} = \epsilon e^{-N_0} \frac{e^N H(N)}{H_0} \frac{c_{s0}}{c_s(N)}. \tag{79}$$

Hence, the parameter ϵ always comes in the combination ϵe^{-N_0}. Since N_0 is arbitrary, we can conveniently choose, e.g., $N_0 = 0$ or a negative number of order $\ln \epsilon$. Hence, the dependence on ϵ may be eliminated by choosing a negative N_0 of order 10, e.g., $N_0 = \ln 0.001 = -6.9$.

For $N_0 = 0$, we have

$$a_0 H_0 = \epsilon c_{s0} q_{\rm CMB}, \tag{80}$$

the horizon crossing relation (78) becomes

$$a_0 e^N H(N) = c_s(N) q, \tag{81}$$

and the condition (77) becomes

$$\epsilon e^{N_{q_{\rm CMB}}} \frac{H(N_{q_{\rm CMB}})}{H_0} \frac{c_{s0}}{c_s(N_{q_{\rm CMB}})} = 1. \tag{82}$$

4.1.1. Rough Estimates

During slow-roll inflation, the Hubble rate H and the sound speed c_s change much slower than the scale factor. In this regime, choosing $N_{\rm in} = 0$ and using (82), we have a rough estimate for $N_{q_{\rm CMB}}$ at the horizon crossing

$$N_{q_{\rm CMB}} \simeq \ln \frac{1}{\epsilon} = 6.9. \tag{83}$$

Using (73) and (82), we also find an estimate for the initial $N_{{\rm in},q_{\rm CMB}}$ of the perturbation with $q = q_{\rm CMB}$

$$N_{{\rm in},q_{\rm CMB}} \simeq \ln \frac{\beta}{\epsilon} = 2.3. \tag{84}$$

Similarly, for any $q \geq q_{\rm CMB}$, we find an order of magnitude estimate for N_q at the horizon crossing

$$N_q \simeq \ln \frac{1}{\epsilon} \frac{q}{q_{\rm CMB}} = 6.9 + \ln \frac{q}{q_{\rm CMB}}, \tag{85}$$

and for the initial $N_{{\rm in},q}$

$$N_{{\rm in},q} \simeq \ln \frac{\beta}{\epsilon} \frac{q}{q_{\rm CMB}} = 2.3 + \ln \frac{q}{q_{\rm CMB}}. \tag{86}$$

If we chose $N_{\rm in} = \ln \epsilon = -6.9$, everything would be shifted by -6.9, and we would obtain

$$N_{q_{\rm CMB}} \simeq 0, \tag{87}$$

$$N_{{\rm in},q_{\rm CMB}} \simeq \ln \beta = -4.6, \tag{88}$$

$$N_q \simeq \ln \frac{q}{q_{\rm CMB}}, \tag{89}$$

and

$$N_{\mathrm{in},q} \simeq \ln \beta \frac{q}{q_{\mathrm{CMB}}} = -4.6 + \ln \frac{q}{q_{\mathrm{CMB}}}. \tag{90}$$

It is convenient to use a new function, sometimes referred to as the Mukhanov–Sasaki variable, $v_q = z\zeta_q$ instead of ζ, where the quantity z is defined by (67). By making use Equations (74) and (80), Equation (68) may be written as

$$v_q'' + (1-\varepsilon_1)v_q' + \left(\frac{e^{-2N}}{\epsilon^2} \frac{c_{\mathrm{s}}^2}{c_{\mathrm{s}0}^2} \frac{H_0^2}{H^2} \frac{q^2}{q_{\mathrm{CMB}}^2} - (2 - \varepsilon_1 + \frac{\varepsilon_2}{2} - \frac{c_{\mathrm{s}}'}{c_{\mathrm{s}}})(1 + \frac{\varepsilon_2}{2} - \frac{c_{\mathrm{s}}'}{c_{\mathrm{s}}}) \right.$$
$$\left. - \frac{\varepsilon_2 \varepsilon_3}{2} + (\frac{c_{\mathrm{s}}'}{c_{\mathrm{s}}})' \right) v_q = 0, \tag{91}$$

where the prime $'$ denotes a derivative with respect to N and should not be confused with the derivative with respect to the conformal time. The slow-roll parameters are defined as $\varepsilon_1 \equiv -\dot{H}/H^2 = -H'/H$ and $\varepsilon_{i+1} \equiv \dot{\varepsilon}_i/(H\varepsilon_i) = \varepsilon_i'/\varepsilon_i$ for $i > 1$.

To find the spectrum at the horizon crossing, Equation (91) should be integrated for a fixed q up to the e-fold number N_{f}, which satisfies the horizon crossing equation (81). If we fix the initial point at $N_{\mathrm{in}} = 0$ and combine Equations (80) and (81), we obtain

$$N = \ln \frac{1}{\epsilon} \frac{q}{q_{\mathrm{CMB}}} \frac{H_0}{H(N)} \frac{c_{\mathrm{s}}(N)}{c_{\mathrm{s}0}}, \tag{92}$$

which, given q, may be regarded as an algebraic equation for N. The explicit functional dependence $H(N)$ and $c_{\mathrm{s}}(N)$ in (92) is obtained by integrating the background Hamilton equations in parallel with (91). Then, the spectrum $\mathcal{P}_{\mathrm{S}}(q)$ can be plotted using the solutions $\zeta_q(N_{\mathrm{f}})$ at the point N_{f} that satisfies (92) for each q.

More precisely, the calculation of the spectrum proceeds as follows. For a set of fixed N_{in}, e.g., $N_{\mathrm{in}} = 0, 1, 2, 3, \ldots$, we integrate the background equations up to N_{in} to find $H(N_{\mathrm{in}})/H_0$ and $c_{\mathrm{s}}(N_{\mathrm{in}})/c_{\mathrm{s}0}$. Using these, we calculate q/q_{CMB} for each N_{in} from the equation

$$\frac{q}{q_{\mathrm{CMB}}} = \frac{\epsilon}{\beta} \frac{H(N_{\mathrm{in}})}{H_0} \frac{c_{\mathrm{s}0}}{c_{\mathrm{s}}(N_{\mathrm{in}})} e^{N_{\mathrm{in}}}, \tag{93}$$

obtained by combining Equations (73), (74), and (76). Then, we solve (92) for N to find the horizon crossing point N_{f} for each q. Finally, we integrate (91) from N_{in} to N_{f} together with the Hamilton equations and plot $\mathcal{P}_{\mathrm{S}}$ versus q/q_{CMB}, using $\zeta_q(N_{\mathrm{f}})$ for each q/q_{CMB}.

4.1.2. Initial Conditions

To determine the proper initial conditions in the deep subhorizon region, we adopt the standard Bunch–Davies vacuum solution [29]

$$v_q(\tau) = \frac{e^{-ic_{\mathrm{s}}q\tau}}{\sqrt{2c_{\mathrm{s}}q}}, \tag{94}$$

where the conformal time $\tau = \int dt/a$ in the slow-roll regime satisfies

$$\tau = -\frac{1+\varepsilon_1}{aH} + \mathcal{O}(\varepsilon_1^2), \tag{95}$$

with $-qc_{\mathrm{s}}\tau \gg 1$ in the deep subhorizon region. Hence, the initial values of v_q and v_q' at N_{in} are determined by (94), up to an arbitrary phase. The simplest choice is

$$v_{q\mathrm{in}} \equiv v_q(N_{\mathrm{in}}) = \frac{1}{\sqrt{2c_{\mathrm{s}}q}}, \tag{96}$$

$$v'_{q\text{in}} \equiv v'_q(N_{\text{in}}) = -i\frac{c_s q}{a_{\text{in}} H_{\text{in}} \sqrt{2c_s q}}. \tag{97}$$

Then, according to (73), we set

$$a_{\text{in}} H_{\text{in}} = \beta q c_s, \tag{98}$$

so

$$v'_{q\text{in}} = -i\frac{1}{\beta\sqrt{2c_s q}}. \tag{99}$$

It is understood that the function c_s in Equations (96)–(99) is taken at $N = N_{\text{in}}$.

4.2. Redefinition of the Input Parameters and Fields

In our calculations, we assume certain values of the parameters and initial values of the fields. In addition, a solution to Equation (91) involves the Bunch–Davies initial conditions (96) and (97). These initial conditions determine the normalization of $\zeta_q(N)$, which in turn fixes the normalization of $\mathcal{P}_S$. Hence, there is a priori no guarantee that the obtained spectrum will satisfy the condition (72). Instead, the calculated value of the spectrum $\mathcal{P}_S(q)$ at the point $q = q_{\text{CMB}}$ will satisfy

$$\mathcal{P}_S(q_{\text{CMB}}) = \frac{A_s}{c_0}, \tag{100}$$

where c_0 is a constant, generally $c_0 \neq 1$. Thus, we have a conflict between the imposed Bunch–Davies vacuum and the normalization of the spectrum to the observed value at the CMB pivot scale.

To rectify this conflict, we need an appropriate redefinition of the input parameters by making use of the scaling invariance of the background equations. To begin, we multiply $\mathcal{P}_S$ by c_0 and write

$$\mathcal{P}_S = c_0\frac{q^3}{2\pi^2}|\zeta_q(N_q)|^2 = \frac{c_0 H^2}{4\pi^2\varepsilon_1 M_{\text{Pl}}^2} q|v_q|^2, \tag{101}$$

where we have used Equations (67) and (69). Now, we absorb c_0 in H^2 and rescale the Hubble rate as $H \to c_0^{-1/2}H$. Note that this rescaling does not affect Equation (91) and its solution v_q because each term in (91) is invariant when multiplying H by a constant. This invariance can easily be verified by checking term by term. The term containing H/H_0 is invariant since H_0 scales in the same way as H. Likewise, the quantities $\varepsilon_1 \equiv -H'/H$, $\varepsilon_2 \equiv \varepsilon_1'/\varepsilon_1$, and $\varepsilon_3 \equiv \varepsilon_2'/\varepsilon_2$ are also invariant when multiplying H by a constant. Finally, the sound speed and its derivatives are not affected due to (28) with (19).

Thus, we obtain a properly normalized spectrum without the c_0 factor. However, when rescaling H, we need to redefine the model's input parameters and background field initial values. Using the scale invariance (44) (Model A) or (56) (Model B) of the background, we infer a redefinition of the parameters. If we repeat the calculations using the redefined input parameters V_0, λ and the initial values rescaled according to (44) in Model A or (56) in Model B, we will obtain the power spectrum that agrees with the observed value at the CMB pivot scale.

4.3. Approximate Spectrum

In the slow-roll regime, the curvature spectrum can be approximated by (see, e.g., Ref. [27])

$$\mathcal{P}_S(q) \simeq \frac{1}{8\pi^2 c_s \varepsilon_1}\frac{H^2}{M_{\text{Pl}}^2}, \tag{102}$$

where for each q, the quantities H, c_s, and ε_1 take on their horizon crossing values at the corresponding N. The approximate spectrum obtained in this way will not, in general,

have the correct observed value at the pivot scale $q_{\rm CMB}$. To satisfy the proper normalization of $\mathcal{P}_{\rm S}(q)$ at $q = q_{\rm CMB}$, we can introduce a constant factor $\bar{c}_0$. To wit, we define

$$\mathcal{P}_{\rm S}(q) \simeq \frac{\bar{c}_0}{8\pi^2 c_{\rm s}\varepsilon_1}\frac{H^2}{M_{\rm Pl}^2}, \tag{103}$$

and fix $\bar{c}_0$ so that $\mathcal{P}_{\rm S}(q_{\rm CMB})$ has the correct observed value at the CMB pivot scale. However, a choice $\bar{c}_0 \neq 1$ will generally violate the assumed Bunch–Davies asymptotic behavior. As before, this problem can be solved by absorbing $\bar{c}_0$ in H^2 and redefining the physical parameters in such a way that the equation for the approximate spectrum reads as in (102). Repeating the procedure of Section 4.2, we redefine the parameters and fields as in Equation (44) (Model A) or Equation (56) (Model B), in which c_0 is replaced by $\bar{c}_0$.

The constants c_0 and $\bar{c}_0$ need not be necessarily equal. However, if we want to compare the exact with the approximate spectrum, we have to stick to the same parameterization of the model in both exact and approximate calculations. In this case, we will replace $\bar{c}_0$ in (103) by c_0 so that the redefinition of parameters and initial values will be the same. Obviously, in this case, the approximate spectrum will fail to reproduce the correct observed value at $q = q_{\rm CMB}$.

4.4. Integration of the Mukhanov–Sasaki Equation

To integrate Equation (68) in conjunction with the Hamilton equations, we need to choose a specific model. By way of example, we present here the spectra calculated for two specific models representing, respectively, classes A and B. Class A will be represented by the PLLS model of Ref. [17] with the Lagrangian (34) in which $\alpha = 1.5$. Class B will be represented by the tachyon Lagrangian (57). In both models, we will use a potential with an inflection point proposed in Ref. [17]

$$U(\lambda\varphi) = V(\lambda\varphi) - V(0), \tag{104}$$

where

$$V(\lambda\varphi) = \ell^4 V_0 \exp\left(-\frac{|\kappa - \lambda\varphi|^n \mathrm{sgn}(\kappa - \lambda\varphi)}{\ell^n M_{\rm Pl}^n}\right). \tag{105}$$

The quantity V_0 is a constant of the dimension of mass to the fourth power. The dimensionless constant κ corresponds to a shift $\phi_0 = \lambda^{-1}\ell^{-2}\kappa$ of the physical field ϕ.

Owing to the inflection point of the potential at $\varphi = \kappa/\lambda$, the scalar field will exhibit an extended flat region for about 30 e-folds. In this flat region, slow-roll conditions will not hold, and inflation will enter into a temporary ultra-slow-roll regime. During this period, the non-constant mode of the curvature fluctuations, which would decay exponentially in the slow-roll regime, actually grows in the ultra-slow-roll regime, enhancing in this way the curvature power spectrum at specific scales that can potentially collapse, forming primordial BHs in the early Universe (for details, see Ref. [17]).

4.4.1. Input Parameters

The initial curvature perturbations will eventually collapse to form BHs if the peak in the amplitude exceeds a certain threshold that strongly depends on the spectrum shape [20]. A desirable spectrum requires the tuning of the input parameters and initial values. To this end, we will use the parameterization of Ref. [17] and fix $\ell = 10^6 M_{\rm Pl}^{-1}$, $n = 3$, $V_0 = 10^{-16} M_{\rm Pl}^4$, and $\lambda = 1.961 \cdot 10^{-8} M_{\rm Pl}$. Here, we have a slight notation difference compared to Ref. [17]. First, the mass scale M in [17] corresponds to ℓ^{-1} in our notation. Second, the dimensionless quantity $(\lambda\ell)^n$ is identical to the quantity denoted by λ in [17]. Thus, the above chosen $\lambda = 1.961 \cdot 10^{-8} M_{\rm Pl}$ corresponds to $\lambda = 7.54 \cdot 10^{-6}$ of Ref. [17].

Third, the constant shift ϕ_0 of the physical field ϕ is identical to our $\lambda^{-1}\ell^{-2}\kappa$. The remaining input parameters are listed in Table 1 for each model in the columns entitled "original".

Using these parameters, we find that the proper normalization to the CMB pivot value at $q = q_{\rm CMB}$, as discussed before, requires $c_0 = 9.4732 \cdot 10^{10}$ for the PLLS model and $c_0 = 10.972$ for the Tachyon model. Hence, to obtain a correct model parameterization, we need to appropriately redefine the parameters and initial values according to (44) for the PLLS model and (56) for the Tachyon model. The redefined values are provided in Table 1 for each model in the columns entitled "redefined".

Table 1. Input parameters.

	PLLS Model, $\alpha = 1.5$		**Tachyon Model**	
	Original	**Redefined**	**Original**	**Redefined**
$V_0[M_{\rm Pl}^4]$	10^{-16}	$9.4732 \cdot 10^{-6}$	10^{-16}	$1.0972 \cdot 10^{-15}$
$\lambda[M_{\rm Pl}]$	$1.961 \cdot 10^{-8}$	$1.324 \cdot 10^{-6}$	$1.961 \cdot 10^{-8}$	$6.49561 \cdot 10^{-8}$
$\phi_0[M_{\rm Pl}]$	0.835	0.0124	0.2586	0.0781
$\phi_{\rm in}[M_{\rm Pl}]$	5.3	0.0785	1.1	0.3321
$\eta_{\rm in}$	$-1.53 \cdot 10^{-8}$	-0.3179	$-3 \cdot 10^{-5}$	$-3.3 \cdot 10^{-4}$

In this way, if we repeat the calculations using the redefined input parameters V_0, λ, and initial values, we will automatically obtain the properly normalized power spectra with no need for the normalization constant c_0. In Figure 1, we plot the curvature power spectra obtained by numerically solving Equation (91), combined with the spectra approximated by Equation (103) for the PLLS and Tachyon models, both with the same potential defined by (104) and (105) and redefined input parameters provided in Table 1.

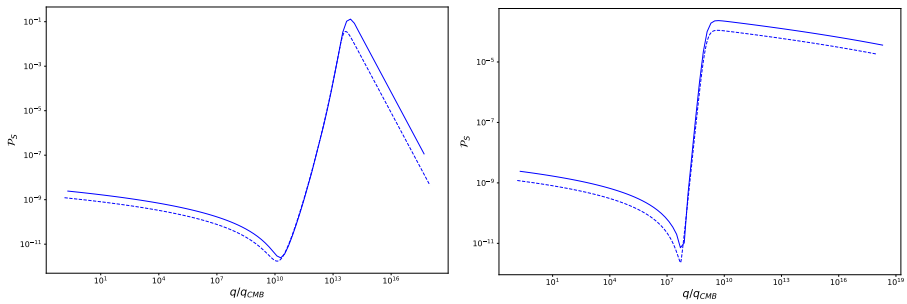

Figure 1. Curvature power spectrum obtained by numerically solving Equation (91) (full line) combined with the spectrum approximated by Equation (103) (dashed line) for the PLLS model (**left panel**) and Tachyon model (**right panel**). The input parameters are provided in Table 1 for each model.

Although we are mainly concerned with power spectrum normalization, it is of considerable interest to explicitly compare the predicted scalar spectral index $n_{\rm S}$ and the tensor-to-scalar ratio r of each model with the current observational constraints. To this end, we compute $n_{\rm S}$ and r for each model for different sets of model parameters and initial values. Since we have not calculated the tensor perturbation spectra, we compute, using the linear approximation in ε-parameters [30],

$$n_{\rm S} \approx 1 - 2\varepsilon_1 - \varepsilon_2, \tag{106}$$

$$r \approx 16 c_s \varepsilon_1, \tag{107}$$

where ε_1 and ε_2 are evaluated at the acoustic horizon of the perturbations with the comoving wavenumber $q_{\rm CMB}$. We have randomly generated many sets of input parameters and initial values in the intervals $0.2 < \phi_0[M_{\rm Pl}] < 0.3$, $10^{-8} < \lambda[M_{\rm Pl}] < 9.9 \cdot 10^{-8}$, $1.0 < \phi_{\rm in}[M_{\rm Pl}] < 1.2$, and $-10^{-4} < \eta_{\rm in} < -9.9 \cdot 10^{-6}$ for the Tachyon model, and $0.75 < \phi_0[M_{\rm Pl}] < 0.9$, $2.7 \cdot 10^{-8} < \lambda[M_{\rm Pl}] < 9.9 \cdot 10^{-8}$, $4.5 < \phi_{\rm in}[M_{\rm Pl}] < 5.5$, and $-10^{-6} < \eta_{\rm in} < -9.9 \cdot 10^{-9}$ for the PLLS model. The parameters V_0 and α given in Table 1 are kept fixed. The resulting value sets for $n_{\rm S}$ and r are collected in the plot in Figure 2, together with observational constraints from Planck 2018 combined data [31].

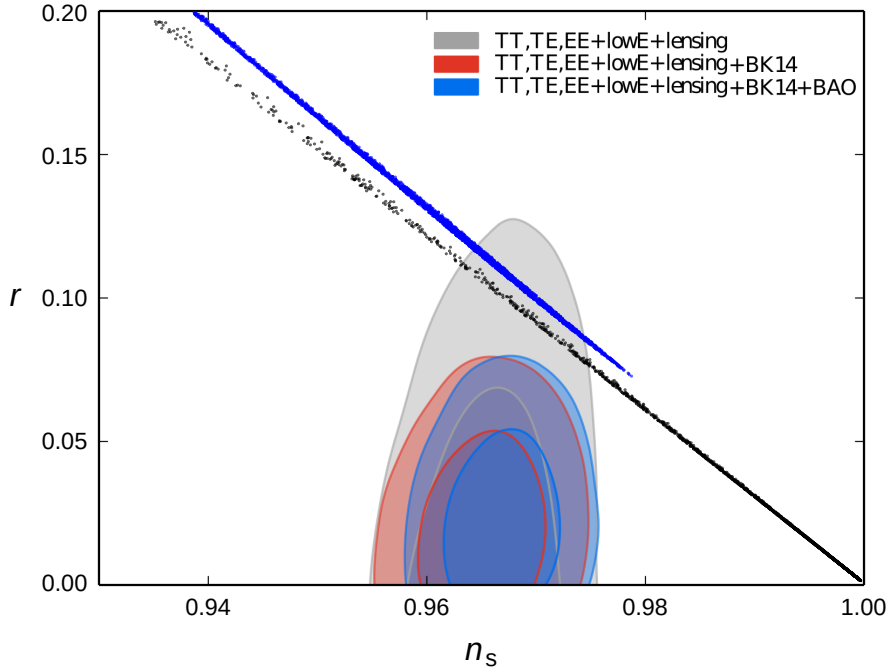

Figure 2. r versus $n_{\rm S}$ diagram with observational constraints from Ref. [31]. The dots represent the theoretical predictions of the PLLS model (blue) and Tachyom model (black). The dots are obtained by varying the parameters ϕ_0 and λ of the potential and initial values $\phi_{\rm in}$ and $\eta_{\rm in}$, as discussed in the text.

The numerical calculations and plots of the power spectrum reveal that the approximate solution is consistently lower by a factor of 3–5. The most discrepancy occurs at the minimum of $P_{\rm S}$. Despite the overall disagreement, the approximate solution captures the essential shape and features of the numerical solution. The disagreement would be much lower if the approximate spectrum were properly normalized to fit the correct value at the CMB pivot scale. In this case, as discussed in Section 4.3, the normalization constant $\bar{c}_0$ would differ from c_0. Consequently, the redefined parameterization would not reproduce the same original model. The main advantage of the approximate solution is that it considerably simplifies and accelerates numerical calculations.

The curvature power spectrum could be fine-tuned to achieve a desirable PBH formation as in single-field inflationary models [32]. IN addition, fine-tuning might be needed to improve the model predictions of observational parameters, such as the spectral index $n_{\rm S}$ and scalar-to-tensor ratio r. Although, in this work, we have not been concerned with this fine-tuning issue, we have checked the sensitivity of the spectra to the input parameters and initial conditions by varying the parameters and initial conditions for the background up to 20%. These variations resulted in transparent and expected changes in the calculated power spectra. Given the initial conditions, the resulting power spectra in both models are smooth and consistent with the approximated power spectrum. As shown in Figure 1, the spectra have transparent shapes with a distinct peak. When the initial conditions are

varied by up to 20%, the spectra exhibit a visible change, particularly at the peak of the power spectrum. The overall shape remains almost unchanged, but the peak's magnitude and position are noticeably affected.

It is important to mention that the backreaction of small-scale one-loop corrections to the large-scale curvature power spectrum could potentially alter the curvature perturbation amplitude measured by Planck. A careful analysis of this backreaction issue, extensively studied in the literature [33–38], would go beyond the scope of our paper. At present, we can only say that one-loop corrections could significantly alter the curvature perturbations in the models studied here. However, since these corrections do not affect the background, the scaling properties still hold, and we believe the input parameters and initial values could be redefined to maintain the correct amplitude at the CMB pivot scale.

4.4.2. Note on the Numerical Routines

We have conducted thorough tests of different numerical integration methods for solving the Hamilton equations and Mukhanov–Sasaki equation, specifically comparing the results from the Runge–Kutta–Fehlberg 7-8, Runge–Kutta Cash–Karp 5-4, and the classic fourth-order Runge–Kutta (RK4) methods. These tests revealed that the average relative differences among these methods' solutions are approximately on the order of 10^{-5}, demonstrating low sensitivity to the choice of the numerical integrator. In all final calculations, we have used the Runge–Kutta-Fehlberg 7-8 method.

5. Summary and Conclusions

We have demonstrated that a general k-essence exhibits a simple scaling property, provided the Lagrangian admits a multiplication by a constant. In particular, we have studied the curvature perturbation spectra for two broad classes of k-inflation models. We have demonstrated that both A and B models enjoy scaling properties, which one can use to tune the model parameters and initial values without affecting the shape of the perturbation spectrum. However, tuning the input parameters, often necessary to achieve the desired properties of the spectrum, will inevitably change the spectrum normalization if one adheres to the Bunch–Davies asymptotic condition.

Using specific representatives of the A and B models, we have shown that our initial choice of input parameters has led to a large disagreement with the observed value at the CMB pivot scale by a factor of the order 10^{11} in the PLLS model and 10 in the Tachyon model. However, owing to the scaling properties, we are allowed to redefine the input parameters in such a way that the spectra keep their shape, satisfy the Bunch–Davies asymptotic, and agree with the observational value at the CMB pivot scale.

We have calculated the scalar spectral index (n_S) and tensor-to-scalar (r) ratio for a large number of sets of input parameters in the two models and presented a comparison with Planck 2018 data. Moreover, we have checked the sensitivity of the curvature power spectrum to the variation of the input parameters and initial conditions.

Our analysis may be useful in the search for inflation models in the context of primordial black-hole production.

Author Contributions: Conceptualization, N.B. and G.S.D.; methodology, N.B.; software, M.M. and M.S.; validation, M.M., M.S. and D.D.D.; formal analysis, G.S.D. and D.D.D. All authors have read and agreed to the published version of the manuscript.

Funding: This research was funded by the Ministry of Science, Technological Development and Innovation of the Republic of Serbia under contracts 451-03-137/2025-03-200113 and 451-03-137/2025-03/200124, and also by ICTP–SEENET-MTP project NT-03 "Theoretical and Computational Methods in Gravitation and Astrophysics–TECOM-GRASP", the COST Action CA1810 "Quantum gravity

phenomenology in the multi-messenger approach" and CEEPUS Program RS-1514-05-2425 "Quantum Spacetime, Gravitation and Cosmology".

Data Availability Statement: No new data were created or analyzed in this study. Data sharing is not applicable to this article.

Acknowledgments: G.S. Djordjević acknowledges the hospitality of the CERN-TH. N. Bilić acknowledges the hospitality of the SEENET-MTP Centre and the Department of Physics, University of Niš, where part of their work was completed.

Conflicts of Interest: The authors declare no conflict of interest. The funding sponsors had no role in the design of the study; in the collection, analyses, or interpretation of data; in the writing of the manuscript; or in the decision to publish the results.

References

1. Armendariz-Picon, C.; Mukhanov, V.F.; Steinhardt, P.J. A dynamical solution to the problem of a small cosmological constant and late-time cosmic acceleration. *Phys. Rev. Lett.* **2000**, *85*, 4438. [CrossRef] [PubMed]
2. Armendariz-Picon, C.; Damour, T.; Mukhanov, V.F. k-inflation. *Phys. Lett. B* **1999**, *458*, 209. [CrossRef]
3. Kamenshchik, A.Y.; Moschella, U.; Pasquier, V. An Alternative to quintessence. *Phys. Lett. B* **2001**, *511*, 265–268. [CrossRef]
4. Bilic, N.; Tupper, G.B.; Viollier, R.D. Unification of dark matter and dark energy: The Inhomogeneous Chaplygin gas. *Phys. Lett. B* **2002**, *535*, 17–21. [CrossRef]
5. Fairbairn, M.; Tytgat, M.H.G. Inflation from a tachyon fluid? *Phys. Lett. B* **2002**, *546*, 1–17. [CrossRef]
6. Frolov, A.V.; Kofman, L.; Starobinsky, A.A. Prospects and problems of tachyon matter cosmology. *Phys. Lett. B* **2002**, *545*, 8. [CrossRef]
7. Shiu, G.; Wasserman, I. Cosmological constraints on tachyon matter. *Phys. Lett. B* **2002**, *541*, 6. [CrossRef]
8. Sami, M.; Chingangbam, P.; Qureshi, T. Aspects of tachyonic inflation with exponential potential. *Phys. Rev. D* **2002**, *66*, 043530. [CrossRef]
9. Shiu, G.; Tye, S.H.H.; Wasserman, I. Rolling tachyon in brane world cosmology from superstring field theory. *Phys. Rev. D* **2003**, *67*, 083517. [CrossRef]
10. Kofman, L.; Linde, A.D. Problems with tachyon inflation. *J. High Energy Phys.* **2002**, *0207*, 004. [CrossRef]
11. Cline, J.M.; Firouzjahi, H.; Martineau, P. Reheating from tachyon condensation. *J. High Energy Phys.* **2002**, *0211*, 041. [CrossRef]
12. Salamate, F.; Khay, I.; Safsafi, A.; Chakir, H.; Bennai, M. Observational Constraints on the Chaplygin Gas with Inverse Power Law Potential in Braneworld Inflation. *Mosc. Univ. Phys. Bull.* **2018**, *73*, 405. [CrossRef]
13. Barbosa-Cendejas, N.; Cartas-Fuentevilla, R.; Herrera-Aguilar, A.; Mora-Luna, R.R.; da Rocha, R. A de Sitter tachyonic braneworld revisited. *J. Cosmol. Astropart. Phys.* **2018**, *2018*, 005. [CrossRef]
14. Dantas, D.M.; da Rocha, R.; Almeida, C.A.S. Monopoles on string-like models and the Coulomb's law. *Phys. Lett. B* **2018**, *782*, 149. [CrossRef]
15. Steer, D.A.; Vernizzi, F. Tachyon inflation: Tests and comparison with single scalar field inflation. *Phys. Rev. D* **2004**, *70*, 043527. [CrossRef]
16. Bilic, N.; Dimitrijevic, D.D.; Djordjevic, G.S.; Milosevic, M.; Stojanovic, M. Tachyon inflation in the holographic braneworld. *J. Cosmol. Astropart. Phys.* **2019**, *08*, 034. [CrossRef]
17. Papanikolaou, T.; Lymperis, A.; Lola, S.; Saridakis, E.N. Primordial black holes and gravitational waves from non-canonical inflation. *J. Cosmol. Astropart. Phys.* **2023**, *03*, 003. [CrossRef]
18. Garcia-Bellido, J.; Morales, E.R. Primordial black holes from single field models of inflation. *Phys. Dark Univ.* **2017**, *18*, 47–54. [CrossRef]
19. Kannike, K.; Marzola, L.; Raidal, M.; Veermäe, H. Single Field Double Inflation and Primordial Black Holes. *J. Cosmol. Astropart. Phys.* **2017**, *09*, 020. [CrossRef]
20. Germani, C.; Musco, I. Abundance of Primordial Black Holes Depends on the Shape of the Inflationary Power Spectrum. *Phys. Rev. Lett.* **2019**, *122*, 141302. [CrossRef]
21. Gibbons, G.W. Thoughts on tachyon cosmology. *Class. Quant. Grav.* **2003**, *20*, S321. [CrossRef]
22. Sen, A. Supersymmetric world volume action for nonBPS D-branes. *J. High Energy Phys.* **1999**, *9910*, 008. [CrossRef]
23. Sen, A. Tachyon matter. *J. High Energy Phys.* **2002**, *07*, 065. [CrossRef]
24. Shandera, S.E.; Tye, S.-H.H. Observing brane inflation. *J. Cosmol. Astropart. Phys.* **2006**, *2006*, 007. [CrossRef]
25. Bilić, N.; Domazet, S.; Djordjevic, G. Tachyon with an inverse power-law potential in a braneworld cosmology. *Class. Quant. Grav.* **2017**, *34*, 165006. [CrossRef]
26. Garriga, J.; Mukhanov, V.F. Perturbations in k-inflation. *Phys. Lett. B* **1999**, *458*, 219–225. [CrossRef]

27. Bertini, N.R.; Bilic, N.; Rodrigues, D.C. Primordial perturbations and inflation in holographic cosmology. *Phys. Rev. D* **2020**, *102*, 123505; Erratum in *Phys. Rev. D* **2022**, *105*, 129901. [CrossRef]
28. De, A.; Mahbub, R. Numerically modeling stochastic inflation in slow-roll and beyond. *Phys. Rev. D* **2020**, *102*, 123509. [CrossRef]
29. Bunch, T.S.; Davies, P.C.W. Quantum Field Theory in de Sitter Space: Renormalization by Point Splitting. *Proc. R. Soc. Lond. A* **1978**, *360*, 117–134. [CrossRef]
30. Lola, S.; Lymperis, A.; Saridakis, E.N. Inflation with non-canonical scalar fields revisited. *Eur. Phys. J. C* **2021**, *81*, 719. [CrossRef]
31. Akrami, Y. et al. [Planck]. Planck 2018 results. X. Constraints on inflation. *Astron. Astrophys.* **2020**, *641*, A10. [CrossRef]
32. Cole, P.S.; Gow, A.D.; Byrnes, C.T.; Patil, S.P. Primordial black holes from single-field inflation: A fine-tuning audit. *J. Cosmol. Astropart. Phys.* **2023**, *08*, 031. [CrossRef]
33. Inomata, K.; Braglia, M.; Chen, X.; Renaux-Petel, S. Questions on calculation of primordial power spectrum with large spikes: the resonance model case. *J. Cosmol. Astropart. Phys.* **2023**, *04*, 011; Erratum in *J. Cosmol. Astropart. Phys.* **2023**, *09*, E01. [CrossRef]
34. Kristiano, J.; Yokoyama, J. Constraining Primordial Black Hole Formation from Single-Field Inflation. *Phys. Rev. Lett.* **2024**, *132*, 221003. [CrossRef]
35. Choudhury, S.; Panda, S.; Sami, M. Quantum loop effects on the power spectrum and constraints on primordial black holes. *J. Cosmol. Astropart. Phys.* **2023**, *11*, 066. [CrossRef]
36. Ballesteros, G.; Egea, J.G. One-loop power spectrum in ultra slow-roll inflation and implications for primordial black hole dark matter. *J. Cosmol. Astropart. Phys.* **2024**, *07*, 052. [CrossRef]
37. Franciolini, G.; Iovino, A., Jr.; Taoso, M.; Urbano, A. Perturbativity in the presence of ultraslow-roll dynamics. *Phys. Rev. D* **2024**, *109*, 123550. [CrossRef]
38. Firouzjahi, H.; Riotto, A. Primordial Black Holes and loops in single-field inflation. *J. Cosmol. Astropart. Phys.* **2024**, *02*, 021. [CrossRef]